Journal of NUCLEAR SCIENCE and TECHNOLOGY, 14[8], pp. 541~550 (August 1977).

Application of Finite Element Method to Two-Dimensional Multi-Group Neutron Transport Equation in Cylindrical Geometry

Toichiro FUJIMURA, Tsuneo TSUTSUI, Kunihiko HORIKAMI, Yasuaki NAKAHARA,

*Japan Atomic Energy Research Institute**

Tadahiro OHNISHI

*Atomic Energy Research Laboratory, Hitachi Ltd.***

Received April 30, 1976
Revised March 3, 1977

The finite element method is applied to the spatial variables of multi-group neutron transport equation in the two-dimensional cylindrical (r, z) geometry. The equation is discretized using regular rectangular subregions in the (r, z) plane. The discontinuous method with bilinear or biquadratic Lagrange's interpolating polynomials as basis functions is incorporated into a computer code FEMRZ. Here, the angular fluxes are allowed to be discontinuous across the subregion boundaries.

Some numerical calculations have been performed and the results indicated that, in the case of biquadratic approximation, the solutions are sufficiently accurate and numerically stable even for coarse meshes. The results are also compared with those obtained by a diamond difference S_n code TWOTRAN-II. The merits of the discontinuous method are demonstrated through the numerical studies.

KEYWORDS: finite element method, neutron transport, cylindrical geometry, Lagrange's interpolating polynomial, Galerkin-type scheme, Crout's method, coarse mesh rebalance, finite difference method, numerical solution, comparative evaluation

I. INTRODUCTION

The finite element method (often simply called FEM) has been well known as a powerful tool to get the numerical solution of many physical problems. It was originally developed in the field of structural analysis[1]. The scope of its applications is now quite diverse and its characteristics, especially in comparison with the finite difference method, have been gradually clarified.

In the field of reactor physics, it has been very popular to use the finite difference method for spatial variables and the discrete ordinate S_n approximation for angular variables. Many computer codes based on the algorithms have been widely used in reactor design and shielding calculations[2]~[4].

On the other hand, the finite element method has not been so much familiar to reactor physicists, but has some advantages over the finte difference method in neutron transport calculations. They are summerized as follows:

(1) Any order of approximation can be achieved by suitable basis functions.
(2) Any complex geometrical configurations can be simulated accurately.
(3) Ray effect familiar to the S_n method can be mitigated through the use of

* *Tokai-mura, Ibaraki-ken.*
** *Ozenji, Tama-ku, Kawasaki-shi.*

angular finite elements.

In 1971 Ohnishi applied the finite element method to the neutron diffusion and transport equations in two-dimensional (x, y) geometries. The triangulation technique is used at first only to the spatial variables[5], and then also to the angular variables in the transport equations[6].

In 1973 Reed *et al.* published a two-dimensional S_n transport code TRIPLET[7] which deals with triangular meshes in planar geometry. During the past several years, some other authors also have developed new finite element techniques to solve neutron diffusion [8]~[10] and transport equations[11]~[17].

In diffusion problems, some real computational advantages over finite difference method have been confirmed for the fast and thermal reactor calculations[9][18], whereas in transport problems, a number of attempts have been made to improve the technique through the use of angular finite elements[11] ~[16], super elements[14] or elements with curved interfaces[17]. Most of them are reviewed and discussed by Froehlich[19] and Gelbard[20].

We have chosen a two-dimensional (r, z) geometry, from a practical point of view and from our intention to proceed further to space dependent kinetics problems. Since only the case of two-dimensional planar[7][13] [15] or one-dimensional geometries[12] have been treated as yet, this work also gives a further insight into the FEM calculations.

The spatial finite element method associated with the angular S_n method is incorporated into a computer code FEMRZ for solving multi-group neutron transport equations in the two-dimensional (r, z) geometry. Main postulations for our formulation are as follows:

(1) We divide the whole system into a number of regular axisymmetric tori, or finite elements, with rectangular cross sectional subregions in the (r, z) plane as shown in **Fig. 1**.

(2) Four and nine nodes are considered in each subregion as illustrated in **Fig. 2**, corresponding to the 1st (bilinear) and the 2nd order (biquadratic) Lagrange's interpolating polynomials, respectively[21].

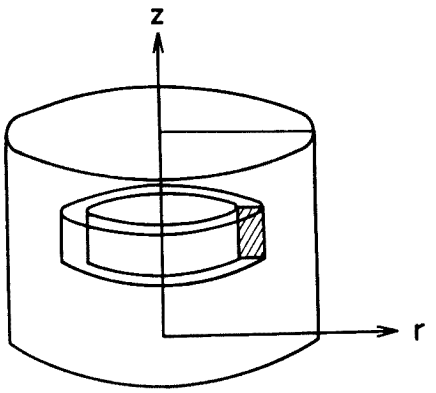

Fig. 1 Definition of rectangular subregion in (r, z) plane

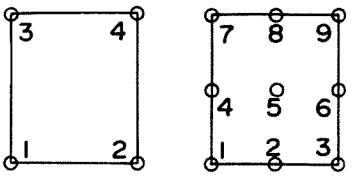

Fig. 2 Node arrangement in subregion for bilinear and biquadratic approximation

(3) Spatial distribution of the angular flux is approximated by a linear combination of these basis functions with coefficients which represent nodal values of the angular fluxes.

(4) The discontinuous method which allows the discontinuity of the angular fluxes at the boundaries of the subregion [7][22] is used.

(5) Galerkin-type scheme in which weight functions are Lagrange's interpolating polynomials themselves is adopted for eliminating the residual, or for yielding a set of algebraic equations for the unknown nodal values of the angular fluxes.

Some modifications and reformulations have been applied to the original formulation [21] for the sake of the convenience of numerical treatments and programming techniques and they are discussed in Chap. IV. Detailed numerical methods are described in Chap. II. Resultant algebraic matrix equations are solved by the Crout's method[23]. Iterations are accelerated by the whole system or coarse mesh rebalance methods. In the latter the rebalance regions are allowed to

be set up arbitrarily.

Several typical calculations are illustrated in Chap. III and the results are compared with those obtained by the diamond difference S_n code TWOTRAN-II[3].

II. SOLUTION ALGORITHMS

Except for geometrical constraints, the computational functions of FEMRZ and physical quantities obtained by it are all the same as those of TWOTRAN-II[3]. Descriptions of boundary condition, convergence criteria *etc.* of FEMRZ are slightly different from, but are specified analogously to TWOTRAN-II.

1. Fundamental Equations

Using the same notations and coordinate system (see **Fig. 3**) as those used in Ref. (3), the time independent two-dimensional transport equation in the (r, z) geometry is written as follows:

$$\frac{\mu}{r}\cdot\frac{\partial(r\psi^g)}{\partial r}-\frac{1}{r}\cdot\frac{\partial(\xi\psi^g)}{\partial\omega}+\eta\frac{\partial\psi^g}{\partial z}+\sigma_t^g\psi^g=S^g,\quad (g=1\sim IGM),\quad (1)$$

where

$$\psi^g=\psi^g(r, z, \mu, \varphi)=\int_{\Delta E_g}\psi(r, z, \mu, \varphi, E)\,dE.$$

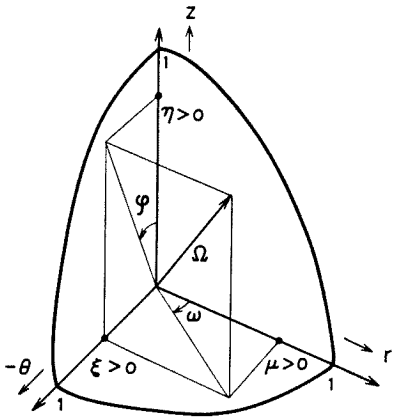

Fig. 3 Angular coordinate system in (r, z) geometry

Under the assumption of the φ-symmetry of the angular flux ψ, we have from Eq. (1)

$$w_m\mu_m\frac{1}{r}\cdot\frac{\partial(r\psi_m^g)}{\partial r}+w_m\eta_m\frac{\partial\psi_m^g}{\partial z}+\frac{1}{r}(\alpha_{m+1/2}\psi_{m+1/2}^g-\alpha_{m-1/2}\psi_{m-1/2}^g)+\sigma_t^g w_m\psi_m^g=w_m S_m^g,\quad (g=1\sim IGM,\ m=1\sim MMT),\quad (2)$$

where the discrete ordinate S_n approximation[3] is used for angular variables. (The unit sphere is partitioned into $2\times MMT$ sections.) Angular dependent quantities are defined by

$$w_m=\iint_{\Delta\Omega_m}d\mu d\varphi\Big/2\pi,$$

$$\psi_m^g=\psi_m^g(r, z)=\Big[\iint_{\Delta\Omega_m}\psi^g(r, z, \mu, \varphi)d\mu d\varphi\Big/2\pi\Big]\Big/w_m,$$

$$\alpha_{m+1/2}=\alpha_{m-1/2}-w_m\mu_m,$$

respectively. Because there is no net particle loss due to angular redistribution, the initial values $\alpha_{m-1/2}$ vanish on each η level in the last equation[3]. (see **Fig. 4**)

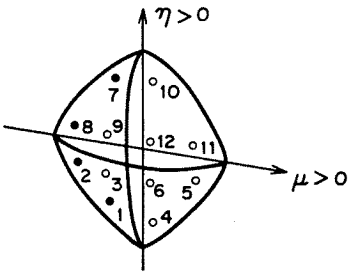

Fig. 4 Order of sweep in discretized angular variable (m) for $MMT=12$ (dark point is a initial sweep angle in each η level)

2. Flux and Source Approximations

Now, let us recall Lagrange's interpolating polynomials. The NP-th order polynomial $L^l(r, z)$ is defined in each rectangular subregion with NPT nodes so that it has the value unity at the l-th node and zero at all the other nodes*. Using these polynomials and coefficients ψ_m^{gl}, we can give an approximate expression $\tilde{\psi}_m^g(r, z)$ to the unknown discretized angular flux $\psi_m^g(r, z)$ in Eq. (2) in the form of a linear combination;

$$\tilde{\psi}_m^g=\sum_{l=1}^{NPT}\psi_m^{gl}L^l.\quad (3)$$

* The NP is the polynomial order in each variable. From the explicit representations which are given in Appendix I of Ref. (21), the polynomial is called here bilinear or biquadratic, corresponding to $NP=1$ or 2, respectively.

This expression is for a local subregion, but we can easily give the global expression by indexing the nodes through the whole system. We, however, need only the local expressions as shown below. The coefficient ϕ_m^{gl} can be interpreted, by definition, as the value of the angular flux at the l-th node. Unknowns are now ϕ_m^{gl}'s, which are determined by a weighted residual method described later on.

Now, we attempt to approximate the source term $S_m^g=S_m^g(r, z)$ in Eq. (2), which is assumed to be known. In preparation for this purpose, let us define moments (the coefficients in spherical harmonics expansion) of nodal flux ϕ_m^{gl} as

$$\phi_{nk}^{gl}=\sum_{m=1}^{MMT} w_m R_{nk}^m \phi_m^{gl}, \quad (k=0\sim n).$$

The functions $R_{nk}^m=R_{nk}(\mu_m, \varphi_m)$ are the spherical harmonics of order n[3]. This implies that the moments of exact angular flux:

$$\phi_{nk}^g=\int_{-1}^{1} d\mu \int_0^{\pi} d\varphi R_{nk}(\mu, \varphi)\psi^g(r, z, \mu, \varphi)/2\pi$$

are approximated by

$$\tilde{\phi}_{nk}^g=\sum_{l=1}^{NPT} \phi_{nk}^{gl} L^l.$$

Under the assumption that related cross sections are constant in the subregion, moments of nodal source are represented (compared with Ref. (3)) as

$$S_{nk}^{gl}=\sum_{g'=1}^{IGM}(2n+1)\sigma_{sn}^{g'\to g}\phi_{nk}^{g'l} + \chi_g \sum_{g'=1}^{IGM} \nu\sigma_f^{g'}\phi_{00}^{g'l}+(2n+1)Q_{nk}^{gl}, \quad (g=1\sim IGM,\ l=1\sim NPT), \quad (4)$$

where the Q_{nk}^{gl}'s are also the nodal values of moments of fixed source. For saving the computer core memory, we store the moments of the fluxes ϕ_{nk}^{gl} instead of the angular fluxes ϕ_m^{gl}. Thus a spherical harmonic expansion of the source term is approximated by

$$\tilde{S}_m^g=\sum_{n=0}^{ISCT}\sum_{k=0}^{n} R_{nk}^m \sum_{l=1}^{NPT} S_{nk}^{gl} L^l, \quad (g=1\sim IGM,\ m=1\sim MMT). \quad (5)$$

Finally, we impose constraints to fluxes in Eq. (2) by the following relation[3]:

$$\phi_{m+1/2}^{gl}=2\phi_m^{gl}-\phi_{m-1/2}^{gl}, \quad (l=1\sim NPT), \quad (6)$$

where the fluxes $\phi_{m-1/2}^{gl}$ are regarded to be known. For the initial angle of the sweep in each η level, an assumption;

$$\phi_m^{gl}=\phi_{m-1/2}^{gl}, \quad (l=1\sim NPT) \quad (7)$$

is used[3].

3. Discontinuous Method with Galerkin-type Scheme

In this section, we describe the solution algorithm for Eq. (2), which is based on the discontinuous method[7][22] and the Galerkin-type scheme. The sweepings of space and angle are made along the neutron flight direction similarly to those of TWOTRAN-II[3].

In the beginning, let us consider an (i, j) subregion;

$$D_{ij}=\{(r, z)\,|\, r_{i-1/2}\leqq r\leqq r_{i+1/2},\ z_{j-1/2}\leqq z\leqq z_{j+1/2}\}$$

which belongs to the i-th interval in the r-direction and the j-th interval in the z-direction*. Let L, R, B and T be the sets formed from the nodes which belong to the left, right, bottom and top boundaries of the D_{ij}, respectively. Two kinds of one variable Lagrange's interpolating polynomials;

$$L_r^l=\begin{cases} L^l(r, z_{j-1/2}) & \text{if } l\in B,\\ L^l(r, z_{j+1/2}) & \text{if } l\in T,\end{cases}$$

$$L_z^l=\begin{cases} L^l(r_{i-1/2}, z) & \text{if } l\in L,\\ L^l(r_{i+1/2}, z) & \text{if } l\in R\end{cases}$$

are constructed from the function L^l.

With the above notations, we define the following three kinds of inner products in the D_{ij}:

$$\langle f, g\rangle=\begin{cases} \iint_{D_{ij}} f\,g\,r\,dr\,dz & \text{if } f\cdot g \text{ is a function of } r \text{ and } z\\ \int_{r_{i-1/2}}^{r_{i+1/2}} f\,g\,r\,dr & \text{if } f\cdot g \text{ is a function of } r\\ \int_{z_{j-1/2}}^{z_{j+1/2}} f\,g\,dz & \text{if } f\cdot g \text{ is a function of } z.\end{cases}$$

The following nine inner products:

$$\langle 1, L^l\rangle,\ \langle L^{l'}, L^l\rangle,\ \langle L^{l'}, \frac{1}{r}L^l\rangle,\ \langle L^{l'}, \frac{\partial}{\partial r}L^l\rangle,$$

* In the local expression, the NPT nodes are arranged in the subregion in the same numbering as shown in Fig. 2.

$\langle L^{l'}, \frac{\partial}{\partial z} L^{l} \rangle$, $\langle 1, L_r^l \rangle$, $\langle L_r^{l'}, L_r^l \rangle$, $\langle 1, L_z^l \rangle$, $\langle L_z^{l'}, L_z^l \rangle$

are enough for working with the discontinuous method with Galerkin-type scheme. Furthermore, some relations, for instance,

$$\langle L^{l'}, L^{l} \rangle = \langle L^{l}, L^{l'} \rangle \quad \text{for any pair } (l', l),$$

$$L_z^{l'} = L_z^{l} \quad \text{for facing nodes, } (r_{i-1/2}, z_{l'}) \text{ and } (r_{i+1/2}, z_l)$$

simplify the calculations. (Details are shown in Ref. [21].)

Now, let us return to Eq. (2). Taking account of the possible discontinuity, our approximation procedure (see Eqs. (3), (5) and (6)) defines the residual $R_m^g = R_m^g(r, z)$ of Eq. (2) as follows:

$$\begin{aligned} R_m^g = {} & w_m |\mu_m| r_{i+1/2} \Big[\sum_{l \in R} (\psi_m^{gl} - \psi_m^{g\bar{l}}) \Big] L_z^l (\delta_{d1} + \delta_{d3}) \\ & + w_m |\eta_m| \Big[\sum_{l \in T} (\psi_m^{gl} - \psi_m^{g\bar{l}}) \Big] L_r^l (\delta_{d1} + \delta_{d2}) \\ & + w_m |\mu_m| r_{i-1/2} \Big[\sum_{l \in L} (\psi_m^{gl} - \psi_m^{g\bar{l}}) \Big] L_z^l (\delta_{d2} + \delta_{d4}) \\ & + w_m |\eta_m| \Big[\sum_{l \in B} (\psi_m^{gl} - \psi_m^{g\bar{l}}) \Big] L_r^l (\delta_{d3} + \delta_{d4}) \\ & + w_m \mu_m \sum_{l=1}^{NPT} \psi_m^{gl} \Big(\frac{\partial}{\partial r} L^l \Big) + w_m \eta_m \sum_{l=1}^{NPT} \psi_m^{gl} \Big(\frac{\partial}{\partial z} L^l \Big) \\ & + (\alpha_{m+1/2} + \alpha_{m-1/2}) \sum_{l=1}^{NPT} \psi_m^{gl} \Big(\frac{1}{r} L^l \Big) \\ & + \sigma_t^g w_m \sum_{l=1}^{NPT} \psi_m^{gl} L^l \\ & - (\alpha_{m+1/2} + \alpha_{m-1/2}) \sum_{l=1}^{NPT} \psi_{m-1/2}^{gl} \Big(\frac{1}{r} L^l \Big) - w_m \tilde{S}_m^g , \\ & \qquad (g = 1 \sim IGM,\ m = 1 \sim MMT), \quad (8) \end{aligned}$$

where the $\delta_{dd'}$ are the Kronecker's deltas in which d refers to a direction of the sweeps as shown in **Fig. 5** and the $(\psi_m^{gl} - \psi_m^{g\bar{l}})$ is the difference of two values of the angular fluxes

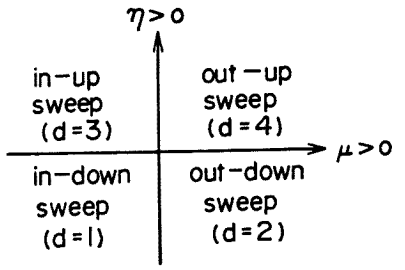

Fig. 5 Value of d corresponding to sweep direction

at the same node l, $\bar{l}$: one defined in the subregion D_{ij} and the other in one of the surrounding subregions.

It is obvious that only two of the first four terms always exist simultaneously for any direction of the sweep (see **Fig. 6**). They give the contribution due to the flux gap and hence disappear in the continuous method[7] [21][22] which does not allow the flux discontinuity.

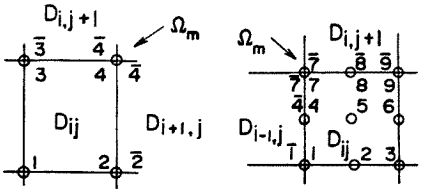

In-down sweep (d=1) in bilinear approximation (NPT=4)

Out-down sweep (d=2) in biquadratic approximation (NPT=9)

Fig. 6 Some allocations of related fluxes on boundaries of subregion D_{ij}

In Eq. (8), the residual R_m^g contains NPT unknowns ψ_m^{gl}, if we assume the outside values $\psi_m^{g\bar{l}}$ to be known already for fixed suffices g, i, j and m. Here, the well-known Galerkin's method

$$\langle L^{l'}, R_m^g \rangle = 0, \quad (l' = 1 \sim NPT) \qquad (9)$$

is applied to yield a set of simultaneous equations of the NPT unknowns. After dividing the Eq. (9) by w_m for simplicity, we get the following NPT dimensional linear system*:

$$\boldsymbol{A}\boldsymbol{\psi} = \boldsymbol{b}. \qquad (10)$$

The explicit expressions of the matrix $\boldsymbol{A} = (a_{l'l})$ and the column vector $\boldsymbol{b} = (b_{l'})$ are;

$$\begin{aligned} a_{l'l} = {} & \mu_m \langle L^{l'}, \frac{\partial}{\partial r} L^l \rangle + \eta_m \langle L^{l'}, \frac{\partial}{\partial z} L^l \rangle + \sigma_t^g \langle L^{l'}, L^l \rangle \\ & + \frac{(\alpha_{m+1/2} + \alpha_{m-1/2})}{w_m} \langle L^{l'}, \frac{1}{r} L^l \rangle \\ & + |\mu_m| r_{i+1/2} \langle L_z^{l'}, L_z^l \rangle (\delta_{d1} + \delta_{d3}) \quad \text{if } l', l \in R \\ & + |\eta_m| \langle L_r^{l'}, L_r^l \rangle (\delta_{d1} + \delta_{d2}) \quad \text{if } l', l \in T \\ & + |\mu_m| r_{i-1/2} \langle L_z^{l'}, L_z^l \rangle (\delta_{d2} + \delta_{d4}) \quad \text{if } l', l \in L \\ & + |\eta_m| \langle L_r^{l'}, L_r^l \rangle (\delta_{d3} + \delta_{d4}) \quad \text{if } l', l \in B, \end{aligned}$$

* This system corresponds to the set of simultaneous equations of all the unknowns in the global expression.

$$b_{l'}=\frac{(\alpha_{m+1/2}+\alpha_{m-1/2})}{w_m}\sum_{l=1}^{NPT}\psi_{m-1/2}\langle L^{l'},\frac{1}{r}L^{l}\rangle$$
$$+\langle L^{l'},\tilde{S}_m^g\rangle$$
$$+|\mu_m|r_{i+1/2}\sum_{l\in R}\psi_m^{gl}\langle L_z^{l'},L_z^{l}\rangle(\delta_{d1}+\delta_{d3}) \quad \text{if } l'\in R$$
$$+|\eta_m|\sum_{l\in T}\psi_m^{g\bar{l}}\langle L_r^{l'},L_r^{l}\rangle(\delta_{d1}+\delta_{d2}) \quad \text{if } l'\in T$$
$$+|\mu_m|r_{i-1/2}\sum_{l\in L}\psi_m^{g\bar{l}}\langle L_z^{l'},L_z^{l}\rangle(\delta_{d2}+\delta_{d4}) \quad \text{if } l'\in L$$
$$+|\eta_m|\sum_{l\in B}\psi_m^{g\bar{l}}\langle L_r^{l'},L_r^{l}\rangle(\delta_{d3}+\delta_{d4}) \quad \text{if } l'\in B,$$
$$(l',l=1\sim NPT).$$

If the suffix m corresponds to the initial angle in each η level, the terms with coefficients α are to be eliminated from both sides of Eq. (10) because of the assumption made in Eq. (7). Thus the formulation of the discontinuous method with Galerkin-type scheme has been established. Here it should be noted that the matrix A is not symmetric.

Before finishing this section, we describe some specifications in FEMRZ code.

(1) Boundary condition: if the top boundary is vacuum, it is specified by

$$\psi_m^{gl}=0 \quad \text{for } \eta_m<0$$

at any node on the top boundary.

(2) The neutron flow crossing, for instance, the right boundary of a subregion from the right to the left is obtained by

$$\sum_{\mu_m<0}w_m\mu_m\Big(\sum_{l\in R}\psi_m^{gl}\langle 1,L_z^{l}\rangle\Big)r_{i+1/2}.$$

It is used in coarse mesh rebalance calculations. In FEMRZ code the rebalancing coarse subregions are taken arbitrarily, whereas in TWOTRAN-II their boundaries must coincide with some material coarse mesh boundaries.

(3) Provision is made for input of the moments Q_{nk}^{gl} of fixed source at each node in a subregion. (see Eq. (4))

(4) Convergence of the inner iteration is tested by

$$\max_{ij}|1-\bar{\phi}_{ij}^{(p-1)}/\bar{\phi}_{ij}^{(p)}|<EPSI,$$

where the $\bar{\phi}_{ij}^{(p)}$ is a scalar flux averaged in the subregion D_{ij} in p-th inner iteration:

$$\bar{\phi}_{ij}=\sum_{l=1}^{NPT}\phi_{00}^{gl}\langle 1,L^{l}\rangle\Big/\iint_{D_{ij}}rdrdz.$$

(5) The Crout's method is used to solve the asymmetric matrix equation, Eq. (10). FEMRZ is not equipped with negative flux control scheme.

III. NUMERICAL EXAMPLES

We have performed calculations for several model and real scale problems while developing the computer code FEMRZ. Problems, for which the conventional S_n calculations are known to yield negative fluxes easily or to show poor convergences, are included to demonstrate the effectiveness of the FEMRZ algorithm compared with the TWOTRAN-II.

Example 1: This is a problem which yields easily negative fluxes in coarse mesh calculations if no recipe for them performed. The configuration is shown in **Fig. 7**. The macroscopic cross sections used for this example are given in **Table 1** (but those of succeeding examples are given in Ref. (24)). The eigenvalue (effective multiplication factor) are calculated varying the number of subregions.

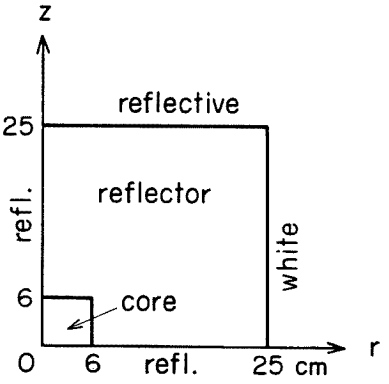

Fig. 7 Model problem configuration and computational conditions for P_0, S_4 and 3-energy-group sample calculations

The solutions shown in **Fig. 8** indicate that the bilinear approximation and the diamond difference scheme give the same order of accuracy, while the biquadratic approximation gives more accurate solutions with coarser meshes. As it is shown in **Table 2**, however, FERMRZ requires now more running cost compared with TWOTRAN-II on the similar computing condition. In the case of 7×7

Table 1 Neutron cross sections (cm^{-1}) of Example 1 (see Fig. 7)

	(a) Core			(b) Reflector		
Group	1	2	3	1	2	3
σ_a	6.26×10^{-2}	6.59×10^{-2}	9.34×10^{-2}	2.91×10^{-2}	7.64×10^{-3}	1.50×10^{-2}
$\nu\sigma_f$	1.51×10^{-1}	1.39×10^{-1}	1.92×10^{-1}	6.54×10^{-2}	3.42×10^{-3}	1.43×10^{-3}
σ_t	2.18×10^{-1}	2.49×10^{-1}	4.56×10^{-1}	2.14×10^{-1}	2.40×10^{-1}	4.56×10^{-1}
σ_{gg}	8.67×10^{-2}	1.61×10^{-1}	3.63×10^{-1}	9.12×10^{-2}	2.04×10^{-1}	4.41×10^{-1}
$\sigma_{g-1,g}$		5.17×10^{-2}	2.20×10^{-2}		7.18×10^{-2}	2.87×10^{-2}
$\sigma_{g-2,g}$			1.71×10^{-2}			2.16×10^{-2}

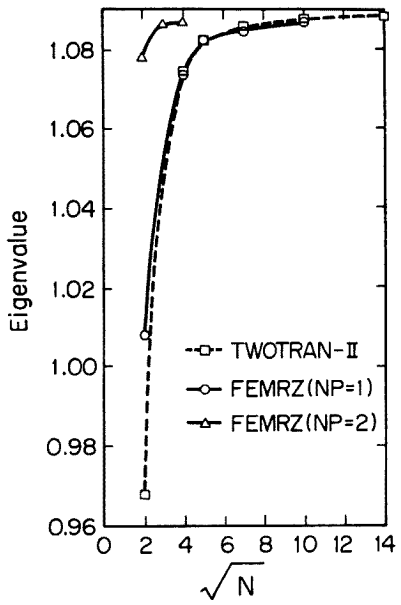

Fig. 8 Dependence of eigenvalue on number of subregions N

Table 2 Running cost of Example 1 on a similar computing condition (see Fig. 8)

Code	TWOTRAN-II	FEMRZ	FEMRZ
Condition	$N=4\times4$	$NP=1$ $N=4\times4$	$NP=2$ $N=2\times2$
Core memory	35,023	51,465	51,054
Time (sec)	4.5	18.6	21.2

subregions bilinear approximation, the negative fluxes are found to appear only in the first outer iteration.

Example 2: This problem is for a fast reactor illustrated in **Fig. 9**, which has a somewhat large core. We present here the first group scalar flux along a radial direction. **Figure 10** shows that the solution based on the biquadratic approximation agrees well with the fine mesh solution obtained by TWOTRAN-II. It may be natural that the coarse mesh solution obtained by TWOTRAN-II can not follow well a correct behavior near the core boundary.

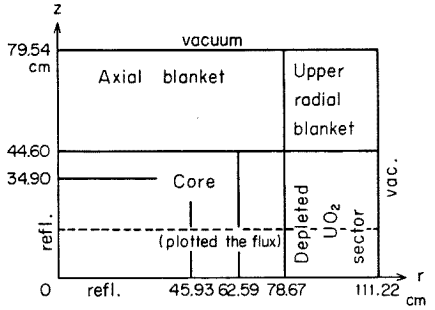

Fig. 9 Fast reactor configuration and computational conditions for P_1, S_4 and 3-energy-group sample calculations

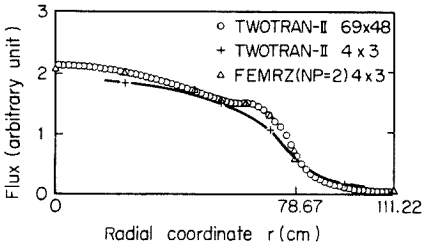

Fig. 10 Comparison of 1st group scalar fluxes along radial direction (see Fig. 9)

It may be worthwhile to mention here one of our experiences on a large heterogeneous thermal reactor with the size of 140 cm×161.5 cm and 13 material regions. The computational conditions were composed of 9-group, P_1, S_8 and average mesh width of 10 cm. The TWOTRAN-II calculation of the system

with uneven coarse meshes failed to converge due to the divergence of the coarse mesh rebalance factors. On the other hand, we have attained the convergence by FEMRZ without regard to the sizes of subregions.

Example 3: The main object in taking up this system shown in **Fig. 11** is to examine the feature of discontinuity at the material boundary where the flux changes steeply.

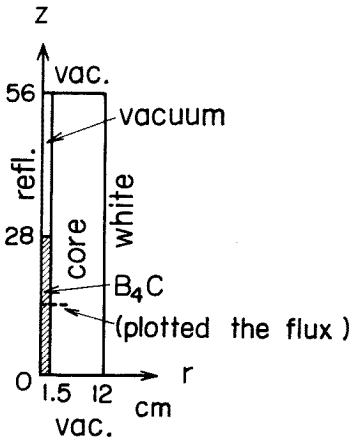

Fig. 11 Reactor configuration containing control rod and computational conditions for P_0, S_4, 2-energy-group sample calculations

Figure 12 shows that the continuous solution of TWOTRAN-II at the B_4C-core boundary

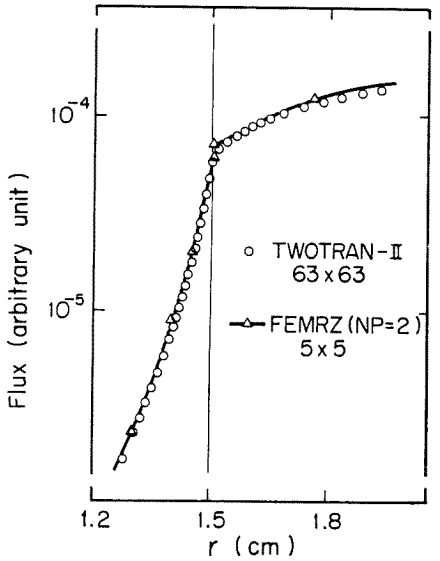

Fig. 12 Comparison of second group scalar fluxes in neighborhood of boundary of control rod (see Fig. 11)

is bounded from above and below by the FEMRZ solutions determined by discontinuous method. The effects of the discontinuity are seen only in the very vicinity of the boundary.

IV. Discussions and Conclusions

In two-dimensional cylindrical geometries, we rarely need to solve neutron transport problems with a complicated geometrical arrangement. Therefore, it is sufficient to use the regular rectangularization to divide the whole system into subregions. This makes it simple also to sweep the region in the direction of the neutron flight.

In the finite element method, arbitrary basis functions can be used. The choice of Lagrange's interpolating polynomials is due to the definiteness of physical meaning of their coefficients and the discrepancy between them at the subregion boundary. A higher order approximation than biquadratic is so complex that the formulation becomes too cumbersome for a practical use. It should be carefully inspected which is more appropriate to use a higher order approximation than biquadratic with coarser meshes, or to employ finer meshes with a lower order approximation.

It is pertinent to explain here about two items which have been taken up in the original formulation[21] but not incorporated into the FEMRZ code. One is a degenerated biquadratic approximation which does not consider the central node. (see Fig. 2) It requires so many arithmetic operations as the usual biquadratic approximation but it may fail to simulate flux distributions with a step peak near the center of a subregion[21]. The other is the continuous method. It has been indicated in Ref. (22) that the method brings into the finite element algorithms the instability due to the appearance of negative fluxes. Whenever the negative fluxes appear some artificial negative flux controls such as "set-flux-to-zero-and-correct" recipe or the use of finer meshes, are necessary to restore the convergence.

The discontinuous method is rather trou-

blesome to formulate and requires relatively a large amount of computer core memory, but it is sufficiently accurate and stable[7][22] as shown in Chap. III. But mathematical foundations of the stability have not been established yet.

As to weight functions, we would be able to choose four polynomials, $1, r, z$ and rz, as TRIPLET for instance, instead of L^1, L^2, L^3 and L^4 in the case of bilinear approximation. But the former choice makes Eq. (9) nearly degenerate, as is shown in the following. For brevity, let us consider the case of quadratic approximation on one-variable r. Each set of the weight functions, then, is $(1, r, r^2)$ and (L_r^1, L_r^2, L_r^3), respectively. **Figure 13** shows that the function r^2 behaves similarly to the r. As can be easily noticed, differences among the successive weight functions become smaller as the order increases. This fact alone sufficiently justifies the application of the Galerkin-type scheme to the residual in the present formulation.

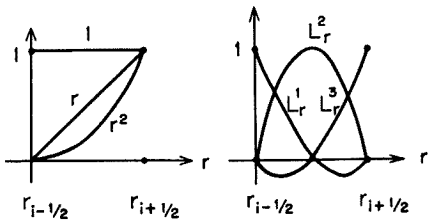

Fig. 13 Two sets of weight functions in quadratic approximation on one variable r

Because the matrix equation, Eq. (10), which is asymmetric and well-conditioned, is to be solved very many times changing the right side of the equation, it is necessary to solve it as quickly as possible. We therefore developed a deviced subroutine based on the no pivoting (on purpose) Crout's method[23]. This leads to a saving of 5 to 10% in computing time.

We are interested in the comparison of the efficiency between the bilinear and biquadratic approximation on the same number of nodes. The eigenvalue and flux calculations of previous examples have ascertained that the latter is more or equally efficient in comparison with the former, as it has been shown also in the case of the triangular mesh for the diffusion problem[9].

We summarize the above discussions as follows:

(1) Optimizations on both computing time and core memory have not yet been completed, so that the FEMRZ code is more time consuming compared with TWOTRAN-II.

(2) Owing to the numerical stability and accuracy, however, the discontinuous method with biquadratic basis functions guarantees reliable results even for coarse meshes chosen not so carefully. On the other hand, as is discussed in Ref. (22), the continuous method does not always give the reliable results for coarse meshes, and its finer mesh calculation may have to be tried depending on the circumstances.

Our efforts will be directed to revise FEMRZ to make it more efficient.

ACKNOWLEDGMENTS

We are much indebted to Dr. T. Asaoka for arrangement of the present work and for many valuable discussions.

We are also thankful to Mr. T. Ise for helpful discussions.

REFERENCES

(1) ZIENKIEWICZ, O.C., CHEUNG, Y.K.: *"The Finite Element Method in Structural and Continuum Mechanics"*, (1967), McGraw-Hill Book Co. Inc., New York, N.Y.
(2) SALTESZ, R.G., *et al.*: *WANL-TMI*-1967, (1967).
(3) LATHROP, K.D., BRINKLY, F.W.: *LA*-4848-*MS*, (1973).
(4) DORSEY, J.P., FROEHLICH, R.: *GA*-8188, (1967).
(5) OHNISHI, T.: Application of finite element solution techniques to neutron diffusion and transport equations, Idaho Falls, Id., *CONF*-710302, Vol. 2, 73 (1971).
(6) *idem*: Finite element solution techniques for neutron transport equations, *Proc. Conf. Numerical Reactor Calculations*, IAEA, Vienna, (1972).
(7) REED, W.H., *et al.*: *LA*-5428-*MS*, (1973).
(8) KANG, C.M., HANSEN, K.F.: *MIT*-3903-5, (1971); *Nucl. Sci. Eng.*, 51[4], 456 (1973).
(9) KAPER, H.G., *et al.*: *ANL*-7925, (1972); *Nucl. Sci. Eng.*, 49[1], 27 (1972).
(10) SEMENZA, L.A., *et al.*: *Nucl. Sci. Eng.*, 47[3], 302 (1972).

(11) UKAI, S.: *J. Nucl. Sci. Technol.*, 9[6], 366 (1972).
(12) MILLER, W.F., Jr., *et al.*: *Nucl. Sci. Eng.*, 51 [2], 148 (1973).
(13) *idem*: *ibid.*, 52[1], 12 (1973).
(14) LEAF, G.K., *et al.*: *ANL*-8052, (1974).
(15) KAPER, H.G., *et al.*: *ANL*-8126, (1974).
(16) YUAN, Y.C., *et al.*: Iterative solution methods for two-dimensional finite element approximations in neutron transport, *Proc. Conf. Computational Methods in Nuclear Engineering*, Charleston, S.C., *CONF*-750413, Vol. 2, III-85 (1975).
(17) LEWIS, E.E., *et al.*: *Nucl. Sci. Eng.*, 58[2], 203 (1975).
(18) DEPPE, L.O., HANSEN, K.F.: *ibid.*, 54[4], 456 (1974).
(19) FROEHLICH, R.: Current problems in multidimensional reactor calculations, *ANS Topical Meeting*, Ann Arbor, Mich., *CONF*-730414, VII -1 (1973).
(20) GELBARD, E.M.: Monte Carlo, finite element and S_n methods, *CONF*-750413, Vol. 2, VII-1 (1975).
(21) HORIKAMI, K., *et al.*: *JAERI-M* 5793, (1974).
(22) REED, W.H., HILL, T.R.: Triangular mesh methods for the neutron transport equation, *CONF* -730414, I-10 (1973).
(23) WESTLAKE, J.R.: "*A Handbook of Numerical Matrix Inversion and Solution of Linear Equations*", (1968), John Wiley & Sons, Inc., New York, N.Y.
(24) FUJIMURA, T., *et al.*: *JAERI-M report*, To be published.